

Void spin distribution as a powerful probe of σ_8

Geonwoo Kang , Jounghun Lee ¹

Department of Physics and Astronomy, Seoul National University,
Kwanak-ro 1, Kwanak-gu, Seoul 08826, Republic of Korea

E-mail: kanggeonwoo@snu.ac.kr, cosmos.hun@gmail.com

Abstract. We present a numerical proof of the concept that the void spin distributions can in principle provide a tight constraint on the amplitude of matter density fluctuation on the scale of $8 h^{-1} \text{Mpc}$ (σ_8) without being severely deteriorated by the degeneracies of σ_8 with cold dark matter density parameter multiplied by the dimensionless Hubble parameter square ($\Omega_{\text{cdm}} h^2$), total neutrino mass (M_ν) and dark energy equation of state (w). Applying the Void-Finder algorithm [1] to a total of 15 AbacusSummit N -body simulations of 15 different cosmological models [2], we identify the giant voids to measure their spins, defined as the magnitudes of rescaled specific angular momenta of void halos. The 15 cosmologies include the Planck ΛCDM and 14 non-Planck models, each of which differs among one another only in one of $\{\sigma_8, \Omega_{\text{cdm}} h^2, M_\nu, w\}$. The probability density distribution of void spins is determined for each model and found to be well approximated by the generalized Gamma distribution with two characteristic parameters, k and θ . It turns out that the best-fit values of k and θ exhibit very sensitive dependences only on σ_8 , being almost insensitive to $\Omega_{\text{cdm}} h^2, M_\nu, w$. This exclusive σ_8 -dependence of the void spin distributions is confirmed to be robust against the variation of the mass and number cuts of void halos. We also test an observational feasibility of estimating the void spins from real data on the galaxy redshifts.

¹Corresponding author.

Contents

1	Introduction	1
2	Identification of voids and measurement of their spins	2
3	Dependence of the void spin distribution on the initial condition	4
3.1	An analytic model for the void spin distribution	4
3.2	Dependence of the void spin distribution on σ_8	6
3.3	Dependences of the void spin distribution on $\Omega_{\text{cdm}}h^2$, M_ν and w	7
4	Observational Feasibility	8
5	Summary and Discussion	12

1 Introduction

The persistent and significant disagreements between the distant and near field probes on the values of the Hubble constant (H_0) and standard deviation of the linear density inhomogeneities on the scale of $8 h^{-1}\text{Mpc}$ (σ_8) have recently drawn considerable attentions [3]. Here, the distant field probe designates the temperature power spectrum of the cosmic microwave background (CMB) radiation, the latest analysis of which yielded $H_0 = 67.36 \pm 0.54$ and $\sigma_8 = 0.811 \pm 0.006$ [4]. Whereas, the near field counterparts are mainly based on the distance-luminosity relation of type Ia supernovae (SNIa) and weak lensing shear two-point correlation functions, which recently yielded the updated results of $H_0 = 73.04 \pm 1.04$ [5] and $\sigma_8 = 0.838^{+0.140}_{-0.141}$ [6]. Although they have yet to blight the legacy of the *concordance* cosmology where the cosmological constant dark energy (DE), Λ , with equation of state $w = -1$ and cold dark matter (CDM) dominate the total energy and matter density of the universe, respectively, these disagreements definitely posed a question on the validity of conventional methodologies and called for a closer scrutiny.

These disagreements between the early and late universe, often called the H_0 and σ_8 tensions, have been addressed by numerous literatures, which can be broadly classified into two categories. In the first category it is claimed that the early-time probes should be much more competent at constraining the initial conditions of the universe, attributing the H_0 and σ_8 tensions to some unknown systematics involved in the near-field probes [7–11]. This claim is refuted by the authors of the secondary category who argue that the late-time probe, as an almost non-parametric approach, should be statistically more reliable than the model dependent early-time probe, interpreting the H_0 and σ_8 tensions as a hint of *new physics* [3, 12–14].

This radical interpretation has recently been boosted up by the result of the Dark Energy Spectroscopic Instrument (DESI) observations that a dynamical dark energy (DE) model with time-varying equation of state, $w(t)$, is preferred to the base ΛCDM one by the Baryonic Acoustic Oscillation (BAO) data combined with the Planck CMB data [15]. Nevertheless, a simple extension of ΛCDM alone is likely to fail in providing a simultaneous solution to the H_0 and σ_8 tensions and to worsen one of them while solving the other [16, 17]. Although it is not so statistically significant as the H_0 tension, the σ_8 tension should not be neglected in

search of a viable new model that is to replace the standard Λ CDM one. In other words, the σ_8 tension ought to be used to constrain further and screen candidate new physics suggested to solve the H_0 tension [17].

In fact, it may require even more meticulous and cautious examinations to resolve the σ_8 tension than the H_0 counterpart given the notorious degeneracy of σ_8 even in the late-time probes with multiple key cosmological parameters such as w and total neutrino mass $M_\nu \equiv \sum m_\nu$ as well as $\Omega_{\text{cdm}}h^2$ with CDM density parameter Ω_{cdm} and dimensionless Hubble constant h . Therefore, before finding a simultaneous solution to both of the tensions, it is quite essential to break the aforementioned cosmological degeneracy by developing new diagnostics that exhibit sensitive dependences mainly on σ_8 . Here, we propose that the probability density functions of void spins may be such a probe on the ground of the results obtained from systematic numerical experiments.

It has been noted for the past two decades that among the large scale structures, the most optimal target for the investigation of the nature of DE and initial conditions is the cosmic voids, almost empty large regions surrounded by filaments and sheets, as their lowest densities make them most susceptible to the acceleration of spacetime. Diverse void properties like their abundance as a function of sizes, ellipticity distributions, density/velocity profiles, and so forth, have been investigated as possible cosmological diagnostics, which indeed revealed that all of them can be useful as a DE discriminator. [18–30]. But, just like the other late-time diagnostics, these void statistics also suffer from the degeneracy among σ_8 , $\Omega_{\text{cdm}}h^2$, M_ν and w [27–29, 31, 32], which could undermine their usefulness as a probe of background cosmology.

In this paper, we are going to numerically prove that the probability distributions of void spins, first defined by ref. [33], depends much more strongly on σ_8 than on $\Omega_{\text{cdm}}h^2$, M_ν and w , and then to assess how feasible it is to estimate this diagnostic in practice. The main contents of the upcoming sections are as follows. In section 2 are presented the descriptions of the numerical dataset, void-identification procedure, and measurements of void spins. In section 3.1 are presented the analytic model for the void spin distributions and explanation for the usage of this formula to quantify the dependence of void spin distributions on the aforementioned four parameters. In section 3.2 are presented the description of strong σ_8 variation of the void spin distributions. In section 3.3 are presented the description of the insensitivities of the void spin distributions to $\Omega_{\text{cdm}}h^2$, M_ν and w . In section 4 is presented a test result of observational feasibility of measuring the void spins from observational data on the redshifts. In section 4 we summarize the results and discuss their implications.

2 Identification of voids and measurement of their spins

Our numerical investigation will be based on the halo catalogs from the AbacusSummit [2], a suite of DM only N -body simulations conducted for a variety of cosmologies including dynamical DE models with time-varying equation of state (w CDM) and mixed DM models with massive neutrinos ($\nu\Lambda$ CDM). The majority of the AbacusSummit simulations was run on a periodic box of a side length $2h^{-1}$ Gpc, keeping tracks of 6912^3 DM particles by implementing the Abacus code [34]. Compared with the conventional cosmological N -body codes, the Abacus code attains unprecedentedly high accuracy and rapidity of computing gravities with the help of a new analytical split method for the force decomposition developed by ref. [35]. The wide scope of initial conditions for all AbacusSummit simulations were all generated with the help of the *Cosmic Linear Anisotropy Solving System* (CLASS) [36].

In the AbacusSummit simulations of $\nu\Lambda$ CDM models are treated the massive neutrinos as continuous fluid elements, whose suppression effects on the growth of structures were incorporated via retracing and rescaling the linear density power spectrum back to $z = 99$ from $z = 1$ [37]. Although no gravitational clustering of massive neutrinos with other particle components were properly taken into account, it was claimed to be a good approximation to the neutrino effects on the scales larger than neutrinos free streaming lengths at higher redshifts before the onset of their nonlinear evolution [2, 37]. Meanwhile, the simulations of w CDM models adopted the simplest parametrization of DE equation of state as $w(z) = w_0 + z w_a / (1 + z)$, assuming no interaction between DE and DM. The gravitationally bound DM halos were resolved in each AbacusSummit simulation via the newly developed COMPASO halo-finding scheme [38, 39], which is an improved version of the conventional spherical overdensity (SO) halo-finder [40]. A detailed description of the COMPASO halo-finder and its comparison with the conventional halo-finders are provided in ref. [38].

For our analysis is chosen a total of 15 different AbacusSummit simulations, whose initial conditions are different from one another only in one of the four cosmological parameters, namely, σ_8 , $\Omega_{\text{cdm}} h^2$, M_ν and w . The choice of these 15 simulations is made through searching for the dataset optimal to the requirements of the current work: the largest box multiple simulations to explore whether or not the void spin distribution can diminish the notorious degeneracies among these four cosmological parameters. Table 1 lists the values of $\Omega_{\text{cdm}} h^2$, σ_8 , M_ν and w , as well as the particle mass resolution (m_p) for the 15 simulations considered here. The other key cosmological parameters are all set at the same Planck values: $n_s = 0.9649$ (spectral index) and $\Omega_b h^2 = 0.024$ (with baryonic matter density parameter Ω_b), and $\Omega_k = 0$ (spatial curvature density parameter). The dimensionless Hubble parameter h , of each AbacusSummit simulation is set at the value that yields the identical CMB acoustic scale [2].

To be consistent with ref. [33] who for the first time introduced the concept of void spins, we identify voids via the Void-Finder algorithm [1] from the halo catalog of each chosen simulation at $z = 0$. For the usage of this algorithm, it is required to specify two parameters, s_c and l_c , which represent the minimum void-size and wall-field halo criterion, respectively [1]. The latter is used to separate the wall halos from the field counterparts, while the former is used to sort out true voids from mere gaps among Poisson distribution of halos [41]. The concise summary of the void-identification procedure based on the Void-Finder algorithm is provided in the below:

- Select the well-resolved DM halos with logarithmic masses larger than a threshold value, $\log [M_c / (h^{-1} M_\odot)] = 11.5$. For each selected halo, locate its third nearest neighbor of each selected halo, and measure the separation distance to it, d_3 . Take the ensemble average over all selected halos, $\langle d_3 \rangle$, and compute its standard deviation, $\sigma_3 \equiv \sqrt{\langle (d_3 - \langle d_3 \rangle)^2 \rangle}$. Determine the value of l_c as $\langle d_3 \rangle + 3\sigma_3/2$. If a halo satisfies the condition of $l_c > d_3$, then classify it as a wall halo.
- Divide the whole simulation box into multiple equal-size grids of side length l_c . Locate a block of empty grids, if any, containing no wall halo, and determine a spherical volume that fits best the block. For each block of empty grids, determine a maximum sphere containing the largest number of empty grids, whose outmost boundary grid just begin to embrace three wall halos.
- Rank the volumes of the empty spheres in a decreasing order, and find the largest empty

sphere in the box to classify it as a maximal (unique void identifier). If the volume of a second largest empty sphere does not overlap with that of the largest maximal by more than 10%, it is classified as another maximal. Iterate this classification with the lower-ranked empty spheres, as far as their radii are larger than s_c .

- Merge the non-maximal spheres into their nearest maximals if their volumes overlap with that of the nearest maximal sphere by more than 50%. This merged region consisting of the maximal and its overlapping non-maximal spheres is finally identified as a void. Using the member halos within the boundary of each void, determine its center of mass and velocity (\mathbf{x}_c and \mathbf{v}_c , respectively).
- Compute the effective radius of each void as $R_{\text{eff}} \equiv (4\pi U_{\text{vol}}/3)^{1/3}$ where the void volume U_{vol} is obtained via the Monte-Carlo simulation method [33]. The residual over-density of each void, δ_v , is also computed as $\delta_v \equiv (n_h - \bar{n}_h)/\bar{n}_h$, where n_h and \bar{n}_h denote the number density of member halos and its mean value, respectively.

The total number of voids N_v , is obviously a function of s_c . It is naturally expected that if s_c is too small, then mere spatial gaps among the halos could be misidentified as voids by the Void-Finder algorithm. To determine a proper value of s_c for the identification of genuine voids, the statistical significance test devised by ref. [41] has to be carried out. Basically, we create 10 Poisson samples consisting of the same number of halos, and find gaps from each sample via the Void-Finder algorithm, and take the average of gap abundance, $N_{\text{gap}}(s_c)$ over the 10 Poisson samples. Finally, the probability defined as $P(s_c) = 1 - N_{\text{gap}}/N_v$, is computed as a function of s_c , which is plotted in figure 1 for the cases of the 15 AbacusSummit simulations. For all of the 15 cosmologies considered in the current work, the statistical significance of void abundance exceed 0.95 [1], if $s_c \geq 8 h^{-1} \text{Mpc}$, which leads us to adopt this universal value of $s_c = 8 h^{-1} \text{Mpc}$ throughout this work. Examples of four giant voids from the simulation of the Planck ΛCDM cosmology (model, c000) are shown in figure 2. Table 2 lists the number of voids (N_v), number of giant voids with 15 or more member halos, mean effective radii (\bar{R}_{eff}), mean halo number density ($\bar{\delta}_h$) and the wall-to-field halo criterion value.

As defined in ref. [33], the dimensionless spin vector, \mathbf{j} , of an identified void is determined as

$$\mathbf{j} \equiv \frac{1}{\sqrt{2}(M_v V_v R_{\text{eff}})} \sum_{i=1}^{n_h} m_i (\mathbf{x}_i - \mathbf{x}_c) \times (\mathbf{v}_i - \mathbf{v}_c). \quad (2.1)$$

Here n_h is the total number of halos inside a given void, $\{m_i, \mathbf{x}_i, \mathbf{v}_i\}$ denote the virial mass, comoving position, and velocity of the i th void halo, respectively, and $V_v \equiv \sqrt{GM_v/R_{\text{eff}}}$ with $M_v \equiv \sum_{i=1}^{n_h} m_i$ and gravitational constant G [42]. Hereafter, the magnitude of this void spin vector, $j \equiv |\mathbf{j}|$, will be referred to as a void spin, as in ref. [33]. Eq. (2.1) indicates that it is not possible to measure a void spin if n_h is too low. The larger number of halos a void has, the more accurately its spin can be measured. In accordance, we apply a halo number cut, $n_c = 15$, to the identified voids from each simulation and exclude those voids with $n_h < n_c$ for the determination of void spin distribution.

3 Dependence of the void spin distribution on the initial condition

3.1 An analytic model for the void spin distribution

Splitting the range of j into multiple short intervals of equal length, Δj , and counting the number, ΔN_v , of voids whose values of j fall in each interval, we determine the probability

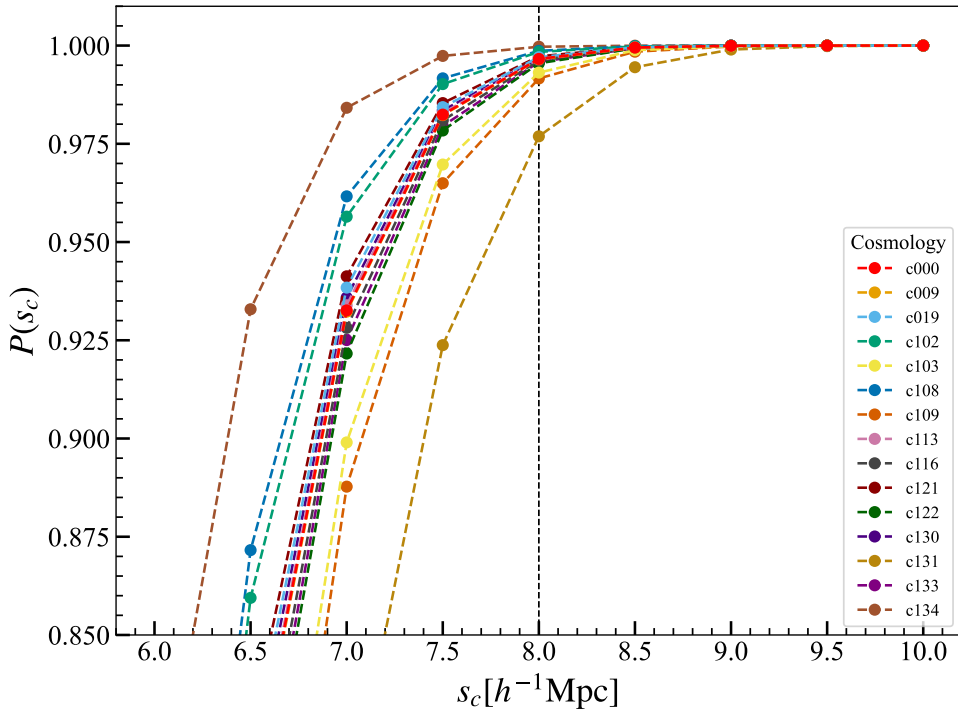


Figure 1. Probabilities that the identified empty regions via the Void-Finder algorithm are not mere gaps among halos but true underdense voids for 15 different cosmological models which differ from one another in one of the four cosmological parameters, σ_8 , $\Omega_{\text{cdm}} h^2$, M_ν and w (see table 1).

density distribution of void spins as $p(j) \equiv \Delta N_v / (N_v \Delta j)$. The errors involved in the measurement of $p(j)$ are computed through the jackknife analysis. Dividing the simulation box into eight smaller boxes of equal volumes and treating those voids belonging to each sub-volume as a jackknife resample, we separately compute the probability density distribution of j for each of the eight resamples. The standard deviation scatter among the eight distribution at each j -interval is determined as the errors in the original value of $p(j)$.

The top panel of figure 3 plots $p(j)$ as black filled circles with the Jackknife errors for the case of the Planck cosmology (c000). As can be seen, just like the well-known spin parameter distribution of galactic halos [42], the void spin distribution, $p(j)$, shows a long high- j tail. Recalling the recent result of ref. [43] that the spin parameter distribution of DM halos was found to be well approximated by the Gamma distribution, we compare the numerically obtained $p(j)$ to the following *generalized* Gamma distribution:

$$p(j) = \frac{j^{k-1}}{2\Gamma\left(\frac{k}{p}\right)\theta^k} \exp\left[-\left(\frac{j}{\theta}\right)^{1/2}\right], \quad (3.1)$$

where $\Gamma(k/p) \equiv \int_0^\infty dt t^{k/p} e^{-t}$, and $\{k, \theta\}$ are two adjustable parameters.

We compare the numerically obtained $p(j)$ with eq. (3.1) via the χ^2 -minimization to determine the best-fit values of $\{k, \theta\}$. The top panel of figure 3 plots the best-fit analytic formula as solid red line, while its bottom panel plots the ratios of the numerical to analytical $p(j)$ values. As can be seen, the generalized Gamma distribution gives a exquisite match

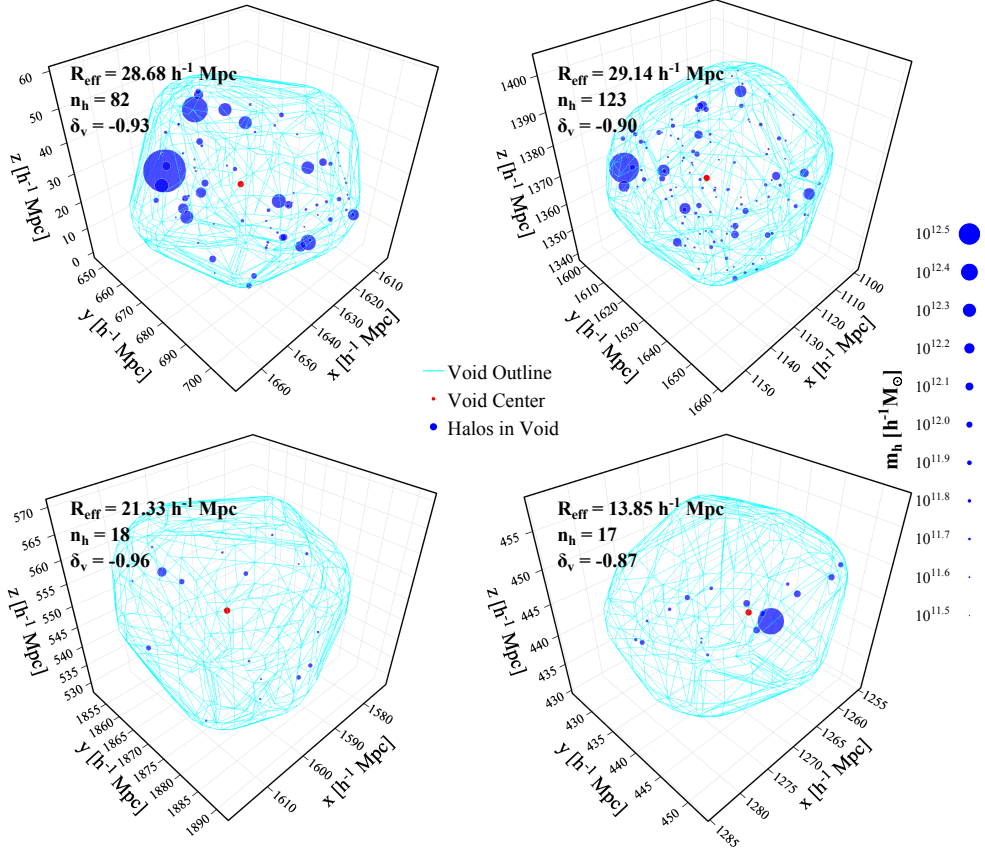


Figure 2. Illustration of four example voids identified via the Void-Finder algorithm from the AbacusSummit simulation of the Planck Λ CDM model with effective radii R_v and number density contrast of void halos δ_v .

to the numerical results in almost entire range of j except for the lowest- j bin ($j < 0.05$), verifying the validity of eq. (3.1) for the Planck Λ CDM case.

3.2 Dependence of the void spin distribution on σ_8

To see if and how the shape and behavior of the void spin distribution, $p(j)$, depend on σ_8 , we repeat the same analysis with the simulations of four different Λ CDM models (c113, c116, c130, and c133), the σ_8 values of which are different from the Planck value, while all of the other cosmological parameters are fixed at the same Planck values. Figure 4 plots the same as figure 3 but for the four different cases of σ_8 . The void spin distribution for the Planck Λ CDM case is also plotted as black dotted line in each panel for comparison. The generalized Gamma distribution, eq. (3.1), turns out to be in good accords with the numerical results of $p(j)$ for all of the four cases of σ_8 .

Each panel of figure 5 plots the contours of 68%, 95% and 99% confidence regions (solid, dashed and dotted lines, respectively) of χ^2 in the two dimensional space spanned by $\{k, \theta\}$ for each case of σ_8 , and compares them with those (red filled contours) of the Planck Λ CDM case (i.e, $\sigma_8 = 0.811$). As can be seen, approximately 10% changes of σ_8 from the Planck value induce highly significant differences in the best-fit values of $\{k, \theta\}$, explicitly demonstrating how sensitively the shape of the void spin distribution depends on σ_8 .

model	σ_8	$\Omega_{\text{cdm}}h^2$	M_ν [eV]	w	m_p [$10^9 h^{-1} M_\odot$]
c000	0.811	0.120	0.06	-1.0	2.00
c113	0.795	0.120	0.06	-1.0	2.00
c116	0.869	0.120	0.06	-1.0	2.00
c130	0.714	0.120	0.06	-1.0	2.00
c133	0.908	0.120	0.06	-1.0	2.00
c102	0.811	0.124	0.06	-1.0	2.06
c103	0.811	0.116	0.06	-1.0	1.94
c131	0.811	0.108	0.06	-1.0	1.83
c134	0.811	0.132	0.06	-1.0	2.17
c009	0.811	0.120	0.00	-1.0	2.00
c019	0.811	0.120	0.12	-1.0	2.00
c108	0.811	0.120	0.06	-0.9	2.00
c109	0.811	0.120	0.06	-1.1	2.00
c121	0.811	0.120	0.06	-0.975	2.00
c122	0.811	0.120	0.06	-1.025	2.00

Table 1. Model, amplitude of the structures, CDM density parameter multiplied by dimensionless Hubble constant square, total neutrinos mass, DE equation of state, and mass resolution.

3.3 Dependences of the void spin distribution on $\Omega_{\text{cdm}}h^2$, M_ν and w

Repeating the same analysis but with four AbacusSummit simulations of four different Λ CDM models (c102, c103, c131 and c134), we also investigate the $\Omega_{\text{cdm}}h^2$ dependence of the void spin distribution, the results of which are shown in figures 6- 7. As can be seen, the void spin distributions exhibit a much weaker dependence on $\Omega_{\text{cdm}}h^2$ than on σ_8 . No statistically significant difference in the best-fit value of $\{k, \theta\}$ is produced even by 10% change of $\Omega_{\text{cdm}}h^2$.

The M_ν -dependence of the void spin distribution is also explored by analyzing in the similar manner the AbacusSummit simulations of two $\nu\Lambda$ CDM models (c009 and c019), the results of which are shown in figures 6-7. As can be seen, the change from the massless neutrino case ($M_\nu = 0$) to the case of twice more massive neutrinos than the Planck value ($M_\nu = 0.12$ eV) does not cause any statistically significant difference in the best-fit value of $\{k, \theta\}$, revealing almost insensitivity of the void spin distribution to the total neutrino mass.

By iterating the same analysis but with four simulations w CDM cosmologies (c108,c109,c121

model	N_v	$N_v(n_h \geq 15)$	\bar{R}_{eff} [$h^{-1}\text{Mpc}$]	$\bar{\delta}_v$	l_c [$h^{-1}\text{Mpc}$]
c000	603034	175702	15.20	-0.87	4.51
c113	602665	175624	15.19	-0.87	4.51
c116	604573	175075	15.28	-0.87	4.53
c130	602169	175783	15.12	-0.87	4.50
c133	606596	174521	15.35	-0.87	4.55
c102	586022	187662	14.81	-0.87	4.41
c103	617829	164184	15.63	-0.87	4.63
c131	639194	142157	16.51	-0.87	4.87
c134	544601	213735	14.07	-0.87	4.20
c009	603674	175321	15.22	-0.87	4.52
c019	599697	178175	15.13	-0.87	4.49
c108	582162	191974	14.73	-0.87	4.37
c109	621515	159426	15.73	-0.87	4.67
c121	597561	179858	15.08	-0.87	4.48
c122	608974	171116	15.35	-0.87	4.56

Table 2. Total number of voids, number of giant voids having ≥ 15 halos, mean effective radii, mean density contrast and criterion distance for the classification of wall halos.

and c122), we inspect the w -dependence of $p(j)$, the results of which are shown in figures 10-11. Since we focus on $z = 0$, we consider only the value of $w_0 = w(z = 0)$ rather than simultaneously considering both of w_a and w_0 . As can be seen, the void spin distribution exhibits quite weak dependence on w whose 10% change yields no statistically significant difference in the best-fit value of $\{k, \theta\}$. Table 3 compiles the best-fit values of $\{k, \theta\}$ with marginalized errors for the 15 cosmologies. Varying the values of halo number and mass cuts, we also repeat the analyses and confirm that these results shown in figures 4-11, i.e., sensitive dependence of the void spin distribution only on σ_8 is quite robust against the variation of n_c and M_c .

4 Observational Feasibility

Now that the potential of void spin distributions as a sensitive probe of σ_8 is verified, we would like to address a critical issue of how feasible it will be in practice to estimate the void

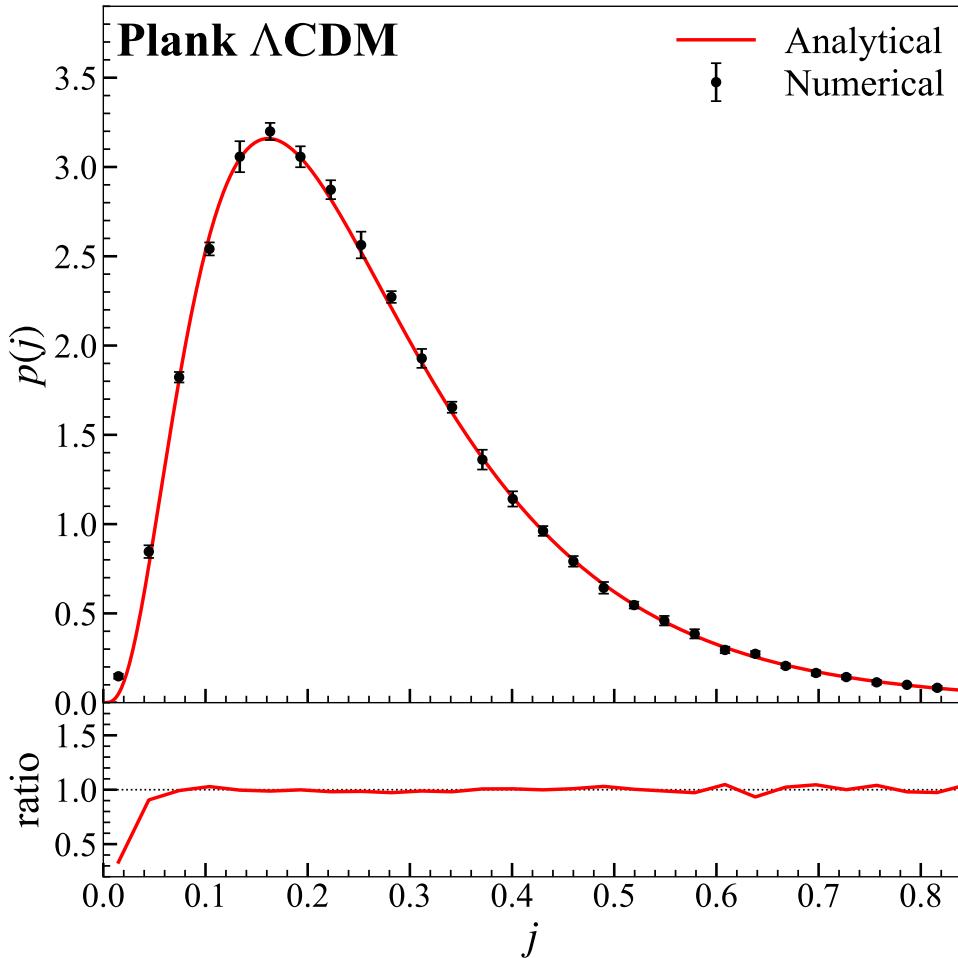


Figure 3. (Top panel): probability density distribution of void spins (black filled circles) with Jackknife errors from the AbacusSummit simulations of the Planck Λ CDM cosmology (c000) and the generalized Gamma distribution with the best-fit parameters (red solid lines); (Bottom panel): ratio of the numerically obtained $p(j)$ to its best-fit analytical model.

spins from real data. The primary hindrance to its observational measurement should come from large uncertainties involved in the measurements of peculiar velocities of void galaxies. To overcome this practical difficulty, it would be desirable to develop a methodology with which the void spins can be observationally estimated even when information on the peculiar velocities of void galaxies is unavailable.

Recollecting the methodology proposed by ref. [44] to statistically determine the filament spins by measuring only the redshifts of filament galaxies, we suggest that it should be applicable to the voids and to estimate their spins. To back up this claim, we follow the procedures [44] in the below. First, for each void, project the positions of its member halos as well as its spin vector onto the x - y plane normal to the $\hat{\mathbf{z}}$ axis, which is assumed to be in the line-of-sight direction. Second, compute the radial components of the velocity vectors of void halos as $\mathbf{v}_r \equiv \hat{\mathbf{z}} \cdot \mathbf{v}$, and take the average, $\langle v_r \rangle$, over all member halos of a given void. Provided that the spin direction of a given void is not perfectly aligned with $\hat{\mathbf{z}}$, the projected

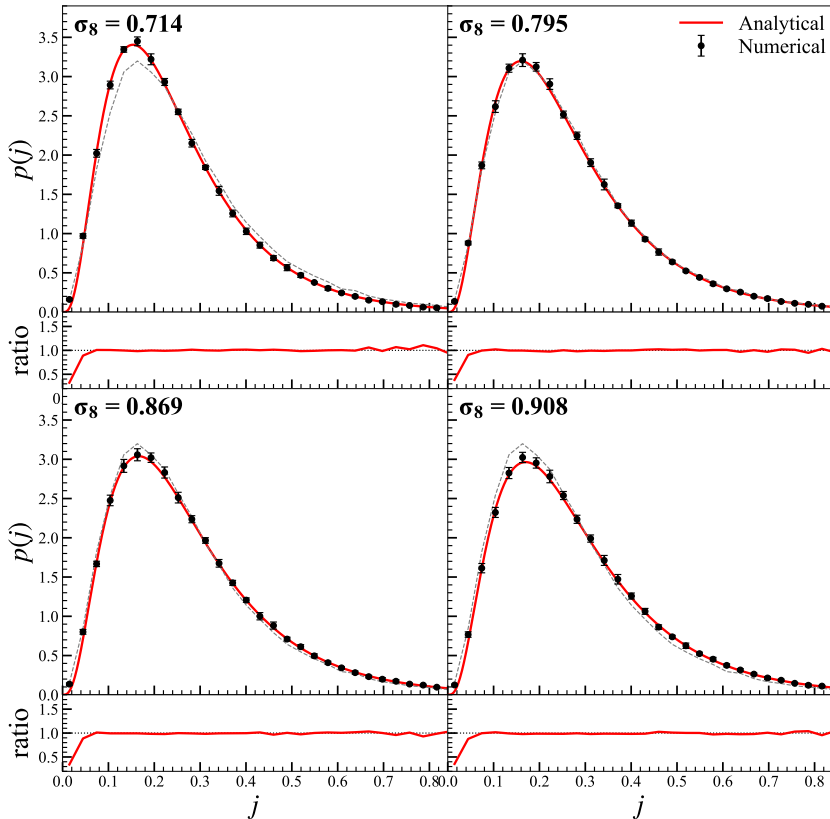


Figure 4. Same as figure 3 but for four different cases of σ_8 .

spin vector, $\mathbf{j}_{2d} \equiv \mathbf{j} \cdot \hat{\mathbf{z}}$, would divide the projected void region into two sectors: one that contains those halos which exhibit $v_r < \langle v_r \rangle$ (blueshifts), while the other that contains those halos with $v_r > \langle v_r \rangle$ (redshifts). Third, reorient the coordinate axes of the projected space to have the direction of \mathbf{j}_{2d} align with its x -axis. The void halos belonging to the region with y -axis coordinate of $y > 0$ ($y < 0$) will exhibit blueshifts (redshifts). Measuring the maximum difference between the blueshifts and redshifts of the member galaxies for each void, which should be proportional to j_{2d} , the probability density distribution, $p(j_{2d})$, can be estimated.

Figure 12 illustrates three projected voids each of which is divided into two sectors by the projected spin vectors (green arrows) aligned with the x -axis, for three different cases of $\cos \phi$ defined as the dot-product between the void spin vectors and line of sight directions. As can be seen, for the case of $\cos \phi \approx 1$ (i.e., the case of a perfect alignment between \mathbf{j} and $\hat{\mathbf{z}}$, the radial velocities of void halos appear to be randomly distributed, showing no mean difference between the two sectors ($y > 0$ and $y < 0$). Whereas, for the case of $\cos \phi < 1$, the radial velocities of void halos exhibit two distinct behaviors, *blueshifts* and *redshifts*, between the two sectors, due to the void spinning motion (curved arrows). The smaller the value of $\cos \phi$ is, the larger the difference between the blueshift and redshift behaviors of the void halos

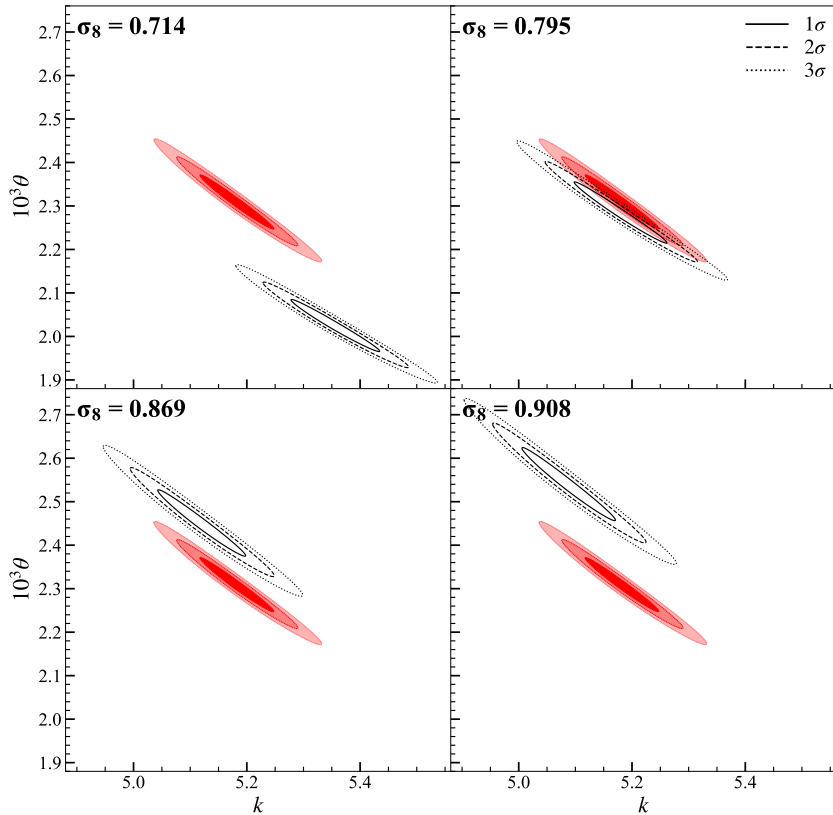


Figure 5. Contours of 68%, 95% and 99% confidence area in the two dimensional configuration space spanned by k and θ for the five different cases of σ_8 . In each panel, the black unfilled contours correspond to the Λ CDM case with a given σ_8 while the red filled contours correspond to the Planck case.

belonging to the two sectors.

Given these examples, we believe that it should be in principle possible to determine the projected void spins in the plane of sky by measuring the observable redshifts of void galaxies and their projected positions, as well, without having any information on the peculiar velocities of void galaxies. In reality, however, there is no available information on the directions of \mathbf{j}_{2d} , which should play the vital role of dichotomizing the void regions into two distinct sectors where the void galaxies yield the maximum blueshift and redshift differences. But, as done in ref. [44], the projected void spin direction could be found through random optimization process, by repeatedly creating a two dimensional direction and computing, Δv_r , which is beyond the scope of this paper.

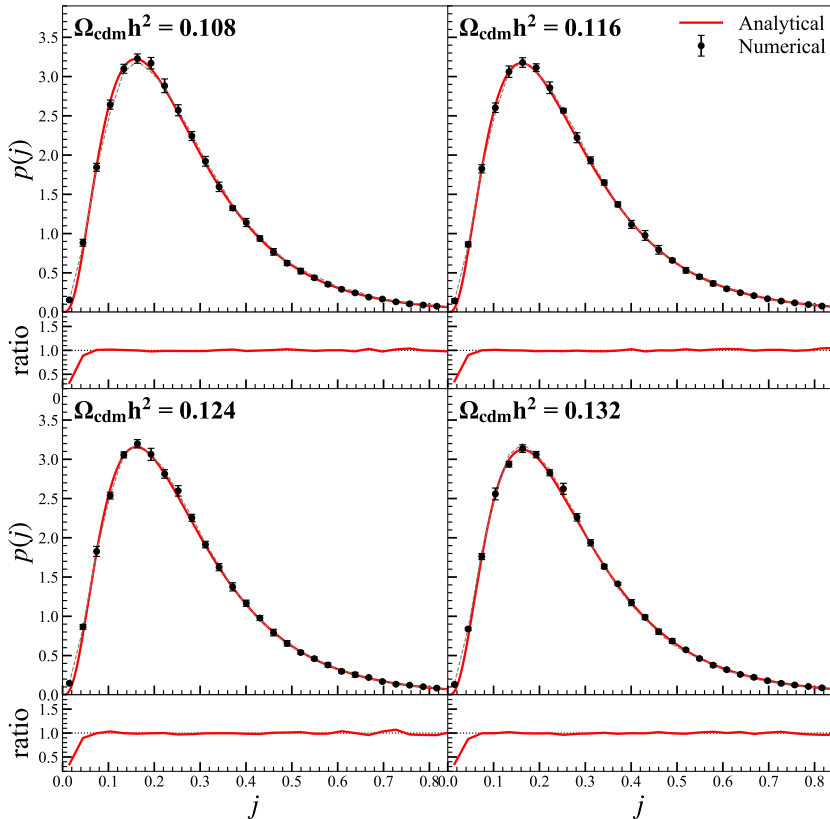


Figure 6. Same as figure 4 but for four different cases of $\Omega_{\text{cdm}}h^2$.

5 Summary and Discussion

With the help of the AbacusSummit simulations which made it achievable to investigate the single parameter dependence of any late-time probe, we have numerically discovered that the void spin distribution has a potential to diminish the degeneracy of σ_8 with $\Omega_{\text{cdm}}h^2$, M_ν and w . From each of 15 different AbacusSummit simulations whose initial conditions are different among one another only in one of the aforementioned four cosmological parameters, the voids have been identified via the Void-Finder algorithm [1] which has an advantage of being directly applicable to the spatial distribution of halos without requiring any assumption on the matter field. The magnitude of the rescaled specific angular momentum of each identified void is determined as a void spin by treating its member halos as component particles. The underlying assumption is that the member halos of a void possess not only radial but also tangential motions relative to its center due to the anisotropic tidal field of surrounding cosmic web [45]. For the measurement of void spin distribution, we have included only those voids containing 15 or more well-resolved halos with masses $\geq 10^{11.5} h^{-1} M_\odot$.

For all of the 15 cosmologies considered in the current work, the void spin distributions

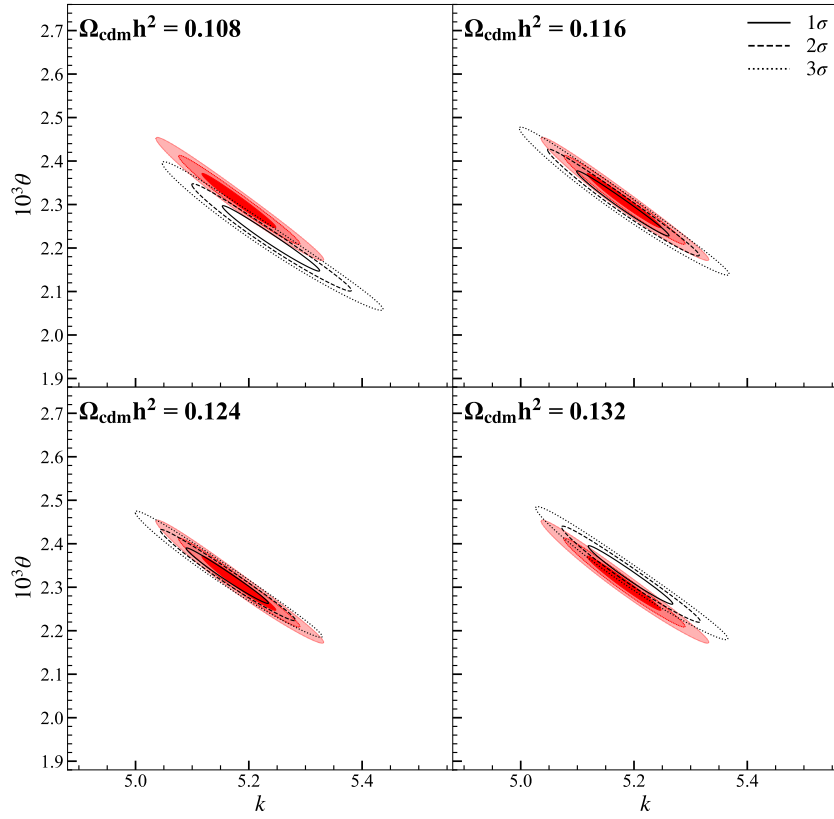


Figure 7. Same as figure 5 but for four different cases of $\Omega_{\text{cdm}}h^2$.

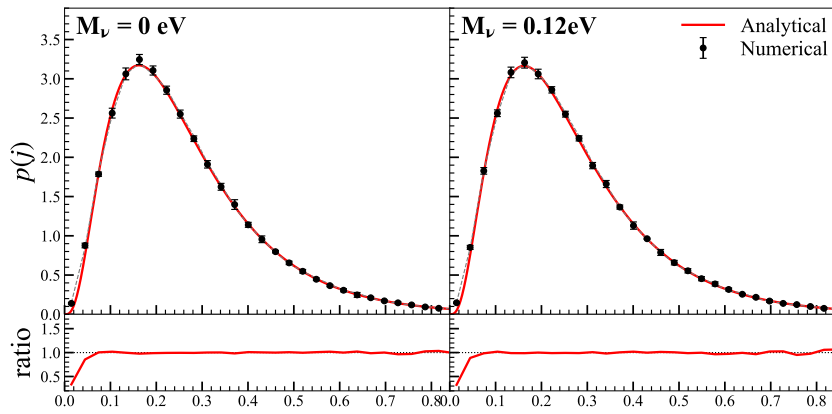


Figure 8. Same as figure 4 but for four different cases of M_ν .

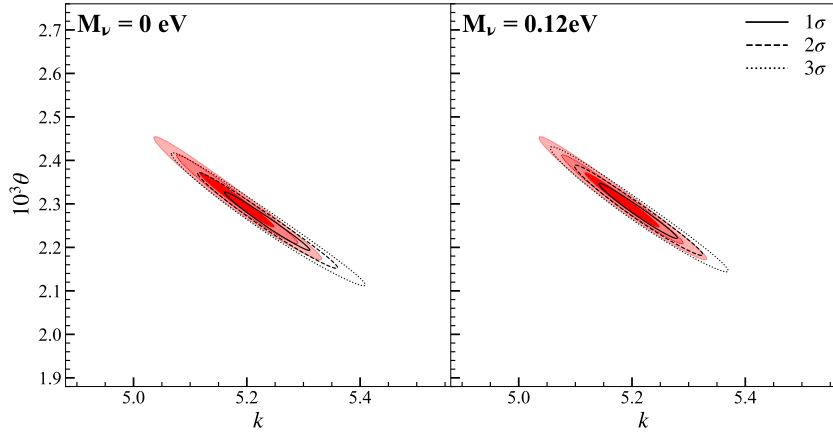


Figure 9. Same as figure 5 but for four different cases of M_ν .

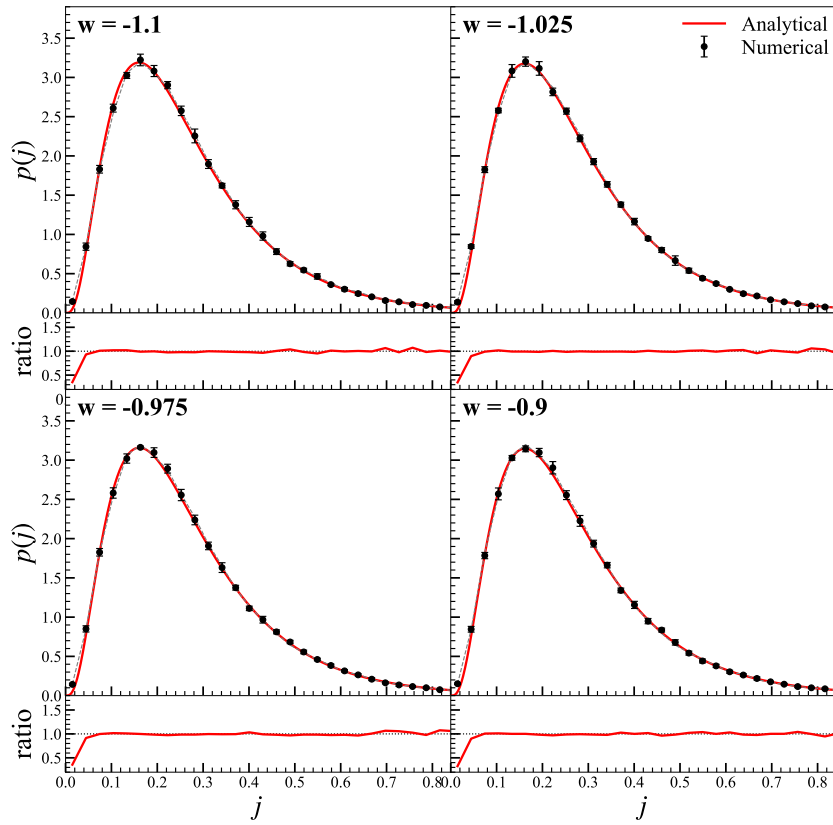


Figure 10. Same as figure 4 but for four different cases of w .

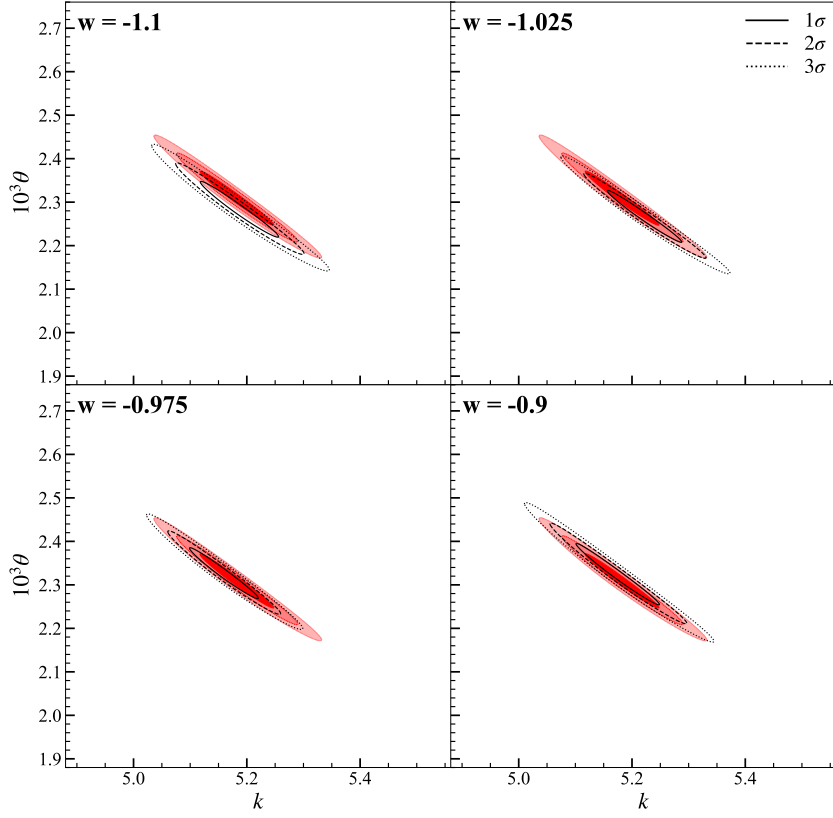


Figure 11. Same as figure 5 for the four different cases of w .

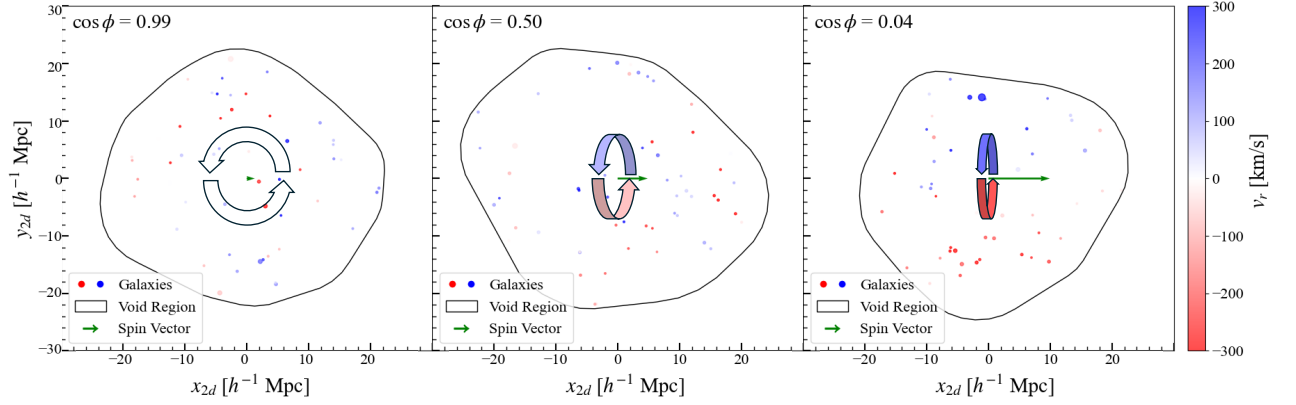


Figure 12. Residual values of the radial components of peculiar velocities of void halos in two dimensional plane orthogonal to the line of sight direction, $\hat{\mathbf{z}}$. Blue dots correspond to the void halos moving toward us while the red dots correspond to the void halos moving away from us, due to their spinning motions.

model	k	$10^3\theta$
c000	$5.175^{+0.048}_{-0.034}$	$2.316^{+0.036}_{-0.044}$
c113	$5.182^{+0.048}_{-0.055}$	$2.280^{+0.053}_{-0.044}$
c116	$5.120^{+0.048}_{-0.055}$	$2.449^{+0.053}_{-0.044}$
c130	$5.347^{+0.062}_{-0.041}$	$2.031^{+0.036}_{-0.044}$
c133	$5.079^{+0.062}_{-0.048}$	$2.547^{+0.044}_{-0.062}$
c102	$5.162^{+0.048}_{-0.048}$	$2.324^{+0.044}_{-0.036}$
c103	$5.182^{+0.048}_{-0.055}$	$2.298^{+0.053}_{-0.044}$
c131	$5.230^{+0.062}_{-0.048}$	$2.227^{+0.053}_{-0.044}$
c134	$5.196^{+0.048}_{-0.055}$	$2.324^{+0.044}_{-0.044}$
c009	$5.230^{+0.055}_{-0.048}$	$2.262^{+0.044}_{-0.044}$
c019	$5.203^{+0.055}_{-0.041}$	$2.289^{+0.036}_{-0.044}$
c108	$5.182^{+0.041}_{-0.055}$	$2.316^{+0.053}_{-0.036}$
c109	$5.189^{+0.041}_{-0.048}$	$2.280^{+0.044}_{-0.036}$
c121	$5.162^{+0.034}_{-0.041}$	$2.324^{+0.044}_{-0.036}$
c122	$5.217^{+0.048}_{-0.041}$	$2.271^{+0.036}_{-0.044}$

Table 3. Best-fit values of k and θ with marginalized errors for the 15 cosmologies.

have been found to be excellently described by the generalized Gamma distribution characterized by two adjustable parameters, $\{k, \theta\}$. The best-fit values of $\{k, \theta\}$ have been determined via the χ^2 statistics and shown to vary significantly with σ_8 , but to exhibit relatively weak dependences on $\Omega_{\text{cdm}}h^2$, M_ν and w . Approximately 10% deviation of σ_8 from the Planck value [4] has turned out to induce a large difference in the best-fit values of $\{k, \theta\}$ as significant as $\geq 5\sigma$. Meanwhile, no such sensitive dependence of $\{k, \theta\}$ on $\Omega_{\text{cdm}}h^2$, M_ν and w has been witnessed. This sensitive σ_8 dependence of the void spin distribution implies that the angular momenta of largest-scale structures, as their third properties, can provide independent information on the initial condition, and thus that they can in principle complement the other cosmological probes based on their first and second properties (i.e., positions and velocities) like the void sizes, shapes and velocity profiles.

It has also been examined how feasible it would be to measure the void spins from real data when only the redshifts of void galaxies are available. Applying to the voids the scheme devised in the heuristic work of ref. [44] to detect the spinning motions of cosmic filaments, we have shown that the void spins can be well estimated in the plane of sky by measuring

only the redshift differences of void galaxies. A success of this scheme, however, is limited to those voids that meet two conditions. First, the spin direction of a given void is not perfectly aligned with the sightline. Second, the void spin is high enough to generate appreciable redshift differences between the member galaxies belonging to the approaching and receding sectors dichotomized by the projected void spin directions.

Although this feasibility test has enhanced a prospect of constraining σ_8 with the void spin distribution in practice, there is still room for improvements both in analytical modeling and numerical tests. First, although the exclusive σ_8 dependence of void spin distribution has been found to be robust in the current work against the variation of mass and number cuts of void halos, it would be more convincing if its robustness against the variation of void finding algorithms is examined and confirmed. Second, although we have provided an analytic formula of the void spin distribution and quantify its σ_8 dependence in terms of the two free parameters of the formula, it will be highly desirable to derive a truly physical model for it from first principles, which will definitely strengthen the void spin distribution as a cosmological diagnostic.

Third, it will be necessary to trace the evolution of the void spin distribution by utilizing light cone simulations and to investigate if it still retains the sensitive σ_8 -dependence even at higher redshifts, where a larger number of voids are available. Tracing the redshift evolution of void spin distribution will also allow us to investigate more completely how the time varying DE equation of state affects the void spin distribution. Fourth, a more thorough investigation of the M_ν dependence of the void spin distribution is required to conclude that this diagnostic is indeed capable of breaking the σ_8 - M_ν degeneracy by taking into account the full nonlinear effects of massive neutrinos as gravitating particles. Our future work will be in the direction of making these improvements.

Acknowledgments

JL acknowledges the support by Basic Science Research Program through the NRF of Korea funded by the Ministry of Education (No.2019R1A2C1083855).

References

- [1] F. Hoyle and M. S. Vogeley, *Voids in the pscz survey and the updated zwicky catalog*, *Astrophys. J.* **566** (2002) 641, doi:10.1086/338340 [arXiv:astro-ph/0109357 [astro-ph]].
- [2] N. A. Maksimova, L. H. Garrison, D. J. Eisenstein, et al., *AbacusSummit: a massive set of high-accuracy, high-resolution N-body simulations*, *Mon. Not. Roy. Astron. Soc.* **508** (2021) 4037, doi:10.1093/mnras/stab2484 [arXiv:2110.11398 [astro-ph.CO]].
- [3] E. Abdalla, G. Franco Abellán, A. Aboubrahim, A. Agnello, O. Akarsu, Y. Akrami, G. Alestas, D. Aloni, L. Amendola and L. A. Anchordoqui, et al. *Cosmology intertwined: A review of the particle physics, astrophysics, and cosmology associated with the cosmological tensions and anomalies*, *JHEAp* **34** (2022) 49, doi:10.1016/j.jheap.2022.04.002 [arXiv:2203.06142 [astro-ph.CO]].
- [4] N. Aghanim et al. [Planck], *Planck 2018 results. VI. Cosmological parameters*, *Astron. Astrophys.* **641** (2020) A6, doi:10.1051/0004-6361/201833910 [arXiv:1807.06209 [astro-ph.CO]].
- [5] A. G. Riess, W. Yuan, L. M. Macri, D. Scolnic, D. Brout, S. Casertano, D. O. Jones, Y. Murakami, L. Breuval and T. G. Brink, et al. *A Comprehensive Measurement of the Local Value of the Hubble Constant with 1 km/s/Mpc Uncertainty from the Hubble Space Telescope*

- and the *SH0ES* Team, *Astrophys. J. Lett.* **934** (2022) L7, doi:10.3847/2041-8213/ac5c5b [arXiv:2112.04510 [astro-ph.CO]].
- [6] M. Asgari *et al.* [KiDS], *KiDS-1000 Cosmology: Cosmic shear constraints and comparison between two point statistics*, *Astron. Astrophys.* **645** (2021) A104, doi:10.1051/0004-6361/202039070 [arXiv:2007.15633 [astro-ph.CO]].
- [7] T. Shanks, L. Hogarth and N. Metcalfe, *Gaia Cepheid parallaxes and 'Local Hole' relieve H_0 tension*, *Mon. Not. Roy. Astron. Soc.* **484** (2019) L64, doi:10.1093/mnrasl/sly239 [arXiv:1810.02595 [astro-ph.CO]].
- [8] C. A. P. Bengaly, U. Andrade and J. S. Alcaniz, *How does an incomplete sky coverage affect the Hubble Constant variance?*, *Eur. Phys. J. C* **79** (2019) 768, doi:10.1140/epjc/s10052-019-7284-4 [arXiv:1810.04966 [astro-ph.CO]].
- [9] E. Mortsell, A. Goobar, J. Johansson and S. Dhawan, *Sensitivity of the Hubble Constant Determination to Cepheid Calibration*, *Astrophys. J.* **933** (2022) 212, doi:10.3847/1538-4357/ac756e [arXiv:2105.11461 [astro-ph.CO]].
- [10] A. Blanchard, J. Y. Héloret, S. Ilić, B. Lamine and I. Tutusaus, *Λ CDM is alive and well*, *Open J. Astrophys.* **7** (2024) 117170, doi:10.33232/001c.117170 [arXiv:2205.05017 [astro-ph.CO]].
- [11] G. Efstathiou, *Evolving Dark Energy or Supernovae Systematics?*, [arXiv:2408.07175 [astro-ph.CO]].
- [12] E. Di Valentino, O. Mena, S. Pan, L. Visinelli, W. Yang, A. Melchiorri, D. F. Mota, A. G. Riess and J. Silk, *In the realm of the Hubble tension—a review of solutions*, *Class. Quant. Grav.* **38** (2021) 153001, doi:10.1088/1361-6382/ac086d [arXiv:2103.01183 [astro-ph.CO]].
- [13] N. Schöneberg, G. Franco Abellán, A. Pérez Sánchez, S. J. Witte, V. Poulin and J. Lesgourgues, *The H_0 Olympics: A fair ranking of proposed models*, *Phys. Rept.* **984** (2022) 1, doi:10.1016/j.physrep.2022.07.001 [arXiv:2107.10291 [astro-ph.CO]].
- [14] A. R. Khalife, M. B. Zanjani, S. Galli, S. Günther, J. Lesgourgues and K. Benabed, *Review of Hubble tension solutions with new *SH0ES* and *SPT-3G* data*, *JCAP* **04** (2024) 059, doi:10.1088/1475-7516/2024/04/059 [arXiv:2312.09814 [astro-ph.CO]].
- [15] A. G. Adame *et al.* [DESI], *DESI 2024 VI: Cosmological Constraints from the Measurements of Baryon Acoustic Oscillations*, [arXiv:2404.03002 [astro-ph.CO]].
- [16] S. J. Clark, K. Vattis, J. Fan and S. M. Koushiappas, *H_0 and S_8 tensions necessitate early and late time changes to Λ CDM*, *Phys. Rev. D* **107** (2023) 083527, doi:10.1103/PhysRevD.107.083527 [arXiv:2110.09562 [astro-ph.CO]].
- [17] L. Heisenberg, H. Villarrubia-Rojo and J. Zosso, *Simultaneously solving the H_0 and σ_8 tensions with late dark energy*, *Phys. Dark Univ.* **39** (2023) 101163, doi:10.1016/j.dark.2022.101163 [arXiv:2201.11623 [astro-ph.CO]].
- [18] J. Lee and D. Park, *Constraining Dark Energy Equation of State with Cosmic Voids*, *Astrophys. J. Lett.* **696** (2009) L10, doi:10.1088/0004-637X/696/1/L10 [arXiv:0704.0881 [astro-ph]].
- [19] R. Biswas, E. Alizadeh and B. D. Wandelt, *Voids as a precision probe of dark energy*, *Phys. Rev. D* **82** (2010) 023002, doi:10.1103/PhysRevD.82.023002 [arXiv:1002.0014 [astro-ph.CO]].
- [20] E. G. P. Bos, R. van de Weygaert, K. Dolag and V. Pettorino, *The darkness that shaped the void: dark energy and cosmic voids*, *Mon. Not. Roy. Astron. Soc.* **426** (2012) 440, doi:10.1111/j.1365-2966.2012.21478.x [arXiv:1205.4238 [astro-ph.CO]].
- [21] G. Lavaux and B. D. Wandelt, *Precision Cosmography with Stacked Voids*, *Astrophys. J.* **754** (2012) 109, doi:10.1088/0004-637X/754/2/109 [arXiv:1110.0345 [astro-ph.CO]].

- [22] E. Massara, F. Villaescusa-Navarro, M. Viel and P. M. Sutter, *Voids in massive neutrino cosmologies*, JCAP **11** (2015) 018, doi:10.1088/1475-7516/2015/11/018 [arXiv:1506.03088 [astro-ph.CO]].
- [23] B. Novosyadlyj and M. Tsizh, *Voids in the Cosmic Web as a probe of dark energy*, Condensed Matter Phys. **20** (2017) 13901, doi:10.5488/CMP.20.13901 [arXiv:1703.00364 [astro-ph.CO]].
- [24] G. Verza, A. Pisani, C. Carbone, N. Hamaus and L. Guzzo, *The Void Size Function in Dynamical Dark Energy Cosmologies*, JCAP **12** (2019) 040, doi:10.1088/1475-7516/2019/12/040 [arXiv:1906.00409 [astro-ph.CO]].
- [25] N. Hamaus, A. Pisani, J. A. Choi, G. Lavaux, B. D. Wandelt and J. Weller, *Precision cosmology with voids in the final BOSS data*, JCAP **12** (2020) 023, doi:10.1088/1475-7516/2020/12/023 [arXiv:2007.07895 [astro-ph.CO]].
- [26] Z. Rezaei, *Dark Matter-Dark Energy Interaction and the Shape of Cosmic Voids*, Astrophys. J. **902** (2020) 102, doi:10.3847/1538-4357/abb59d [arXiv:2010.10823 [astro-ph.CO]].
- [27] C. T. Davies, M. Cautun, B. Giblin, B. Li, J. Harnois-Déraps and Y. C. Cai, *Constraining cosmology with weak lensing voids*, Mon. Not. Roy. Astron. Soc. **507** (2021) 2267, doi:10.1093/mnras/stab2251 [arXiv:2010.11954 [astro-ph.CO]].
- [28] S. Contarini *et al.* [Euclid], *Euclid: Cosmological forecasts from the void size function*, Astron. Astrophys. **667** (2022) A162, doi:10.1051/0004-6361/202244095 [arXiv:2205.11525 [astro-ph.CO]].
- [29] G. Verza, C. Carbone, A. Pisani and A. Renzi, *DEMNUni: disentangling dark energy from massive neutrinos with the void size function*, JCAP **12** (2023) 044, doi:10.1088/1475-7516/2023/12/044 [arXiv:2212.09740 [astro-ph.CO]].
- [30] E. Ebrahimi, *Phenomenological emergent dark energy versus the Λ CDM: ellipticity of cosmic voids*, Mon. Not. Roy. Astron. Soc. **527** (2024) 11962, doi:10.1093/mnras/stad3627.
- [31] D. Park and J. Lee, *The Void Ellipticity Distribution as a Probe of Cosmology*, Phys. Rev. Lett. **98** (2007) 081301, doi:10.1103/PhysRevLett.98.081301 [arXiv:astro-ph/0610520 [astro-ph]].
- [32] E. Fernández-García, J. E. Betancort-Rijo, F. Prada, T. Ishiyama and A. Klypin, *Constraining cosmological parameters using void statistics from the SDSS survey*, [arXiv:2406.13736 [astro-ph.CO]].
- [33] J. Lee and D. Park, *Rotation of Cosmic Voids and Void-Spin Statistics*, Astrophys. J. **652** (2006) 1, doi:10.1086/507936 [arXiv:astro-ph/0606477 [astro-ph]].
- [34] L. H. Garrison, D. J. Eisenstein, D. Ferrer, N. A. Maksimova and P. A. Pinto, *The abacus cosmological N-body code*, Mon. Not. Roy. Astron. Soc. **508** (2021) 575, doi:10.1093/mnras/stab2482 [arXiv:2110.11392 [astro-ph.CO]].
- [35] M. V. L. Metchnik, *A fast N-body scheme for computational cosmology*, Ph.D. Thesis. U. of Arizona (2009)
- [36] J. Lesgourgues, *The Cosmic Linear Anisotropy Solving System (CLASS) I: Overview* (2011) arXiv e-prints. doi:10.48550/arXiv.1104.2932
- [37] L. H. Garrison, D. J. Eisenstein, D. Ferrer, et al., *AbacusSummit: Initial results from a suite of massive N-body simulations*, Mon. Not. Roy. Astron. Soc. **508** (2021) 575, doi:10.1093/mnras/stab2482 [arXiv:2110.11397 [astro-ph.CO]].
- [38] B. Hadzhiyska, D. Eisenstein, S. Bose, L. H. Garrison and N. Maksimova, *compaso: A new halo finder for competitive assignment to spherical overdensities*, Mon. Not. Roy. Astron. Soc. **509** (2021) 501, doi:10.1093/mnras/stab2980 [arXiv:2110.11408 [astro-ph.CO]].
- [39] B. Hadzhiyska, D. J. Eisenstein, S. Bose, et al., *Halo occupation distribution modeling in*

- AbacusSummit simulations*, Mon. Not. Roy. Astron. Soc. **509** (2022) 501, doi:10.1093/mnras/stab2980 [arXiv:2110.11399 [astro-ph.CO]].
- [40] M. S. Warren, P. J. Quinn, J. K. Salmon, W. H. Zurek, *Dark Halos Formed via Dissipationless Collapse. I. Shapes and Alignment of Angular Momentum.*, Astrophys. J. **399** (1992) 405, doi:10.1086/171937
- [41] H. El-Ad and T. Piran, *Voids in the large scale structure*, Astrophys. J. **491** (1997) 421, doi:10.1086/304973 [arXiv:astro-ph/9702135 [astro-ph]].
- [42] J. S. Bullock, A. Dekel, T. S. Kolatt, A. V. Kravtsov, A. A. Klypin, C. Porciani and J. R. Primack, *A Universal angular momentum profile for galactic halos*, Astrophys. J. **555** (2001) 240, doi:10.1086/321477 [arXiv:astro-ph/0011001 [astro-ph]].
- [43] J. S. Moon and J. Lee, *Mutual information between galaxy properties and the initial predisposition*, JCAP **05** (2024) 111, doi:10.1088/1475-7516/2024/05/111 [arXiv:2311.03632 [astro-ph.CO]].
- [44] P. Wang, N. I. Libeskind, E. Tempel, X. Kang and Q. Guo, *Possible observational evidence for cosmic filament spin*, Nature Astron. **5** (2021) 839, doi:10.1038/s41550-021-01380-6 [arXiv:2106.05989 [astro-ph.GA]].
- [45] J. R. Bond, L. Kofman and D. Pogosyan, *How filaments are woven into the cosmic web*, Nature **380** (1996) 603, doi:10.1038/380603a0 [arXiv:astro-ph/9512141 [astro-ph]].
- [46] X. Li, T. Zhang, S. Sugiyama, R. Dalal, R. Terasawa, M. M. Rau, R. Mandelbaum, M. Takada, S. More and M. A. Strauss, *et al. Hyper Suprime-Cam Year 3 results: Cosmology from cosmic shear two-point correlation functions*, Phys. Rev. D **108** (2023) 123518, doi:10.1103/PhysRevD.108.123518 [arXiv:2304.00702 [astro-ph.CO]].
- [47] R. E. Keeley, S. Joudaki, M. Kaplinghat and D. Kirkby, *Implications of a transition in the dark energy equation of state for the H_0 and σ_8 tensions*, JCAP **12** (2019) 035, doi:10.1088/1475-7516/2019/12/035 [arXiv:1905.10198 [astro-ph.CO]].
- [48] K. Jedamzik, L. Pogosian and G. B. Zhao, *Why reducing the cosmic sound horizon alone can not fully resolve the Hubble tension*, Commun. Phys. **4** (2021) 123, doi:10.1038/s42005-021-00628-x [arXiv:2010.04158 [astro-ph.CO]].
- [49] Ö. Akarsu, E. Ó. Colgáin, A. A. Sen and M. M. Sheikh-Jabbari, *Λ CDM Tensions: Localising Missing Physics through Consistency Checks*, Universe **10** (2024) 305, doi:10.3390/universe10080305 [arXiv:2402.04767 [astro-ph.CO]].
- [50] Z. Sakr, *Extensions to Λ CDM at Intermediate Redshifts to Solve the Tensions?*, PoS CORFU2022 (2023) 262, doi:10.22323/1.436.0262 [arXiv:2305.02913 [astro-ph.CO]].